PRL News – The Spectrum

AUGUST 2020

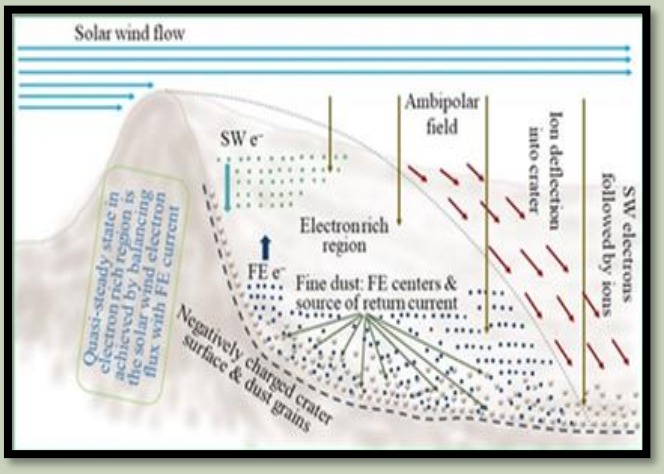

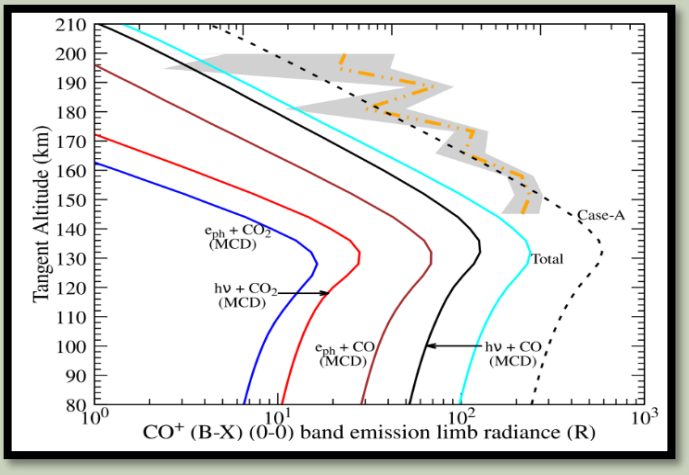

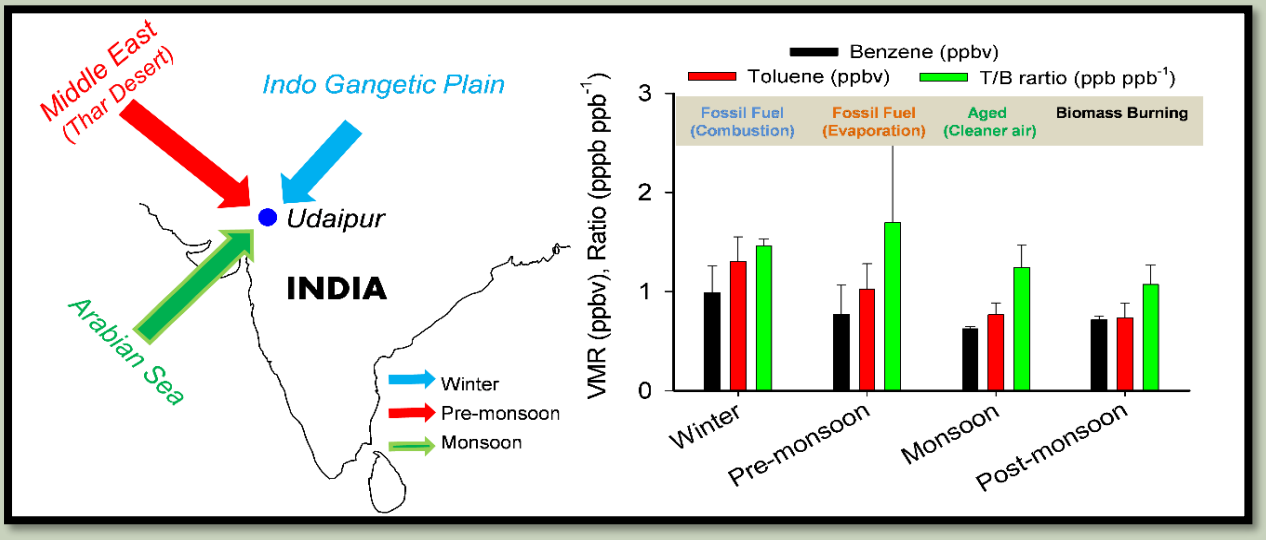

Physical Research Laboratory
Ahmedabad - 380009
India

भौतिक अनुसंधान प्रयोगशाला
अहमदाबाद-380009
भारत

Website: https://www.prl.res.in/prl-eng/newsletter

Contact us: newsletter@prl.res.in

Infrared attenuation due to phase change from amorphous to crystalline observed in astrochemical propargyl ether ices

(K K Rahul, J K Meka, S Pavithraa, P Gorai, A Das, J -I Lo, B N Raja Sekhar, B -M Cheng, P Janardhan, A Bhardwaj, N J Mason, B Sivaraman)(03/04/2020)*

Rahul Kumar

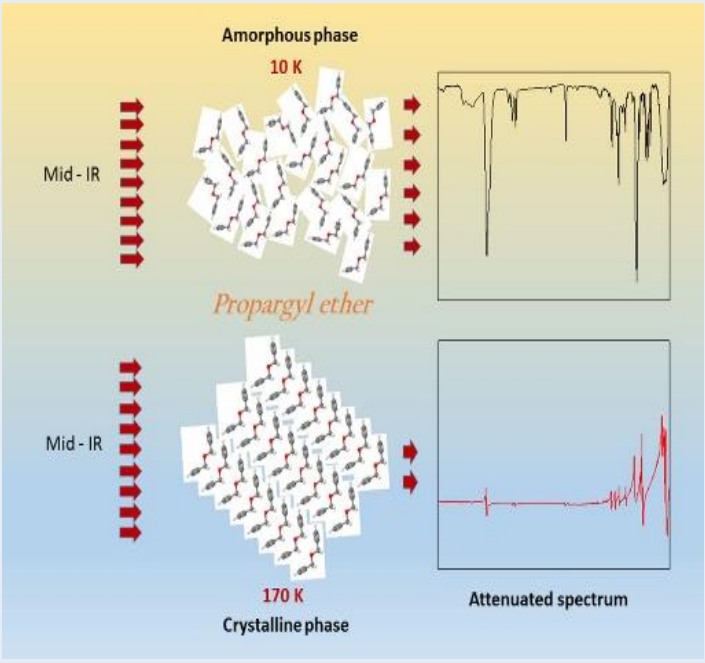

Figure: *Infrared attenuation from crystalline propargyl ether ice at 170 K*

Astrochemical ices are known to undergo morphological changes, from amorphous to crystalline, upon warming the ice from lower (10 K) to higher temperatures. Phase changes are generally identified by the observation of significant changes in the InfraRed (IR) spectrum, where the IR bands that are broad in the amorphous phase are narrower and split when the ice turns crystalline. To-date all the molecules that have been studied under astrochemical conditions, have been observed to show such a behaviour, without significant attenuation at the IR wavelengths. However, in this paper we report a new observation of propargyl ether ($C_3H_3OC_3H_3$). When $C_3H_3OC_3H_3$ is warmed from the amorphous phase, at 10 K, through the phase transition temperature of 170 K, the crystalline ice is found to strongly attenuate IR photons at the mid-IR wavelengths.

https://doi.org/10.1016/j.saa.2019.117393

Residue from Vacuum Ultraviolet Irradiation of Benzene Ices: Insights into the Physical Structure of Astrophysical Dust

(K K Rahul, E Shivakarthik, J K Meka, A Das, V Chandrasekaran, B N Rajasekhar, J- I Lo, B- M Cheng, P Janardhan, A Bhardwaj, N J Mason, B Sivaraman)(15/04/2020)*

We have irradiated benzene ices deposited at 4 K on a cold, interstellar dust analog with vacuum ultraviolet (9 eV) irradiation for periods lasting from several hours to nearly a day, after which the irradiated ice was warmed to room temperature. Vacuum ultraviolet photo-absorption spectra of the aromatic residue left at room temperature were recorded and showed the synthesis of benzene derivatives. The residue was also imaged using an electron microscope and revealed crystals of various sizes and shapes. The result of our experiments suggests such geometrically shaped dust particles may be a key component of interstellar dust.

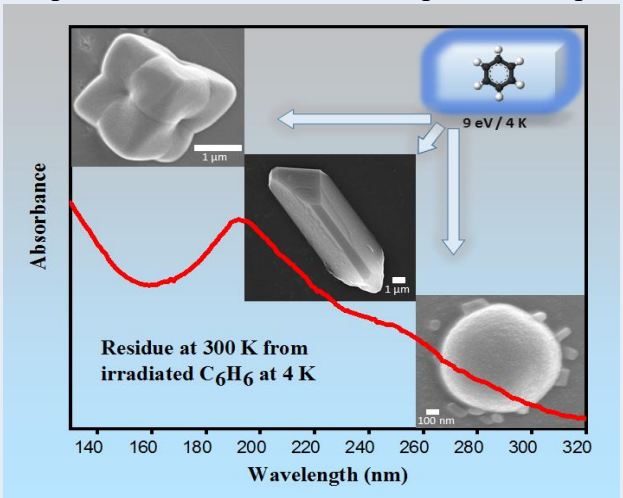

Figure: *FE-SEM image of residue obtained from irradiated benzene ice at 4 K with its VUV spectrum at 300 K.*

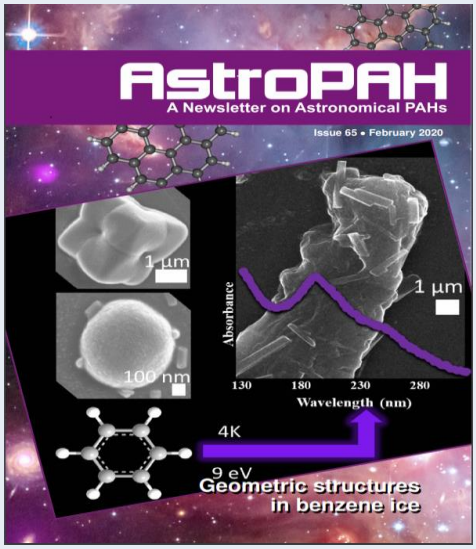

Figure: *Results published on the cover page of the AstroPAH newsletter.*

https://doi.org/10.1016/j.saa.2019.117797

Planetary Remote Sensing Laboratory

(Neeraj Srivastava, Abhishek J. Verma, R.R. Mahajan, K. Acharyya)

Neeraj Srivastava

One of the major goals of planetary remote sensing is to decipher surface composition through reflectance/imaging spectroscopy. In order to aid in the analysis of the remotely acquired data and to assist in detector optimization for future missions a *Planetary Remote Sensing Laboratory* has been established at PRL, Thaltej campus. We plan to carry out reflectance spectroscopy of planetary materials (such as meteorites & returned samples) and analogues under simulated conditions. The measurements will be carried out as a function of fluctuations in viewing geometry, grain size variations, mineral mixtures and changes in environmental conditions. In order to achieve these goals, the following instruments have been installed in the laboratory.

1) An ASD FieldSpec 4 Hires spectroradiometer (350 – 2500 nm)
2) A specifically designed Planetary Environmental Chamber for Reflectance Spectroscopy
3) A custom built Goniometric Assembly suitable for integration with ASD Fieldspec 4 Hires
4) A pulveriser for creating rock powders up to 20 microns
5) A sieve shaker for creating various grain size separates

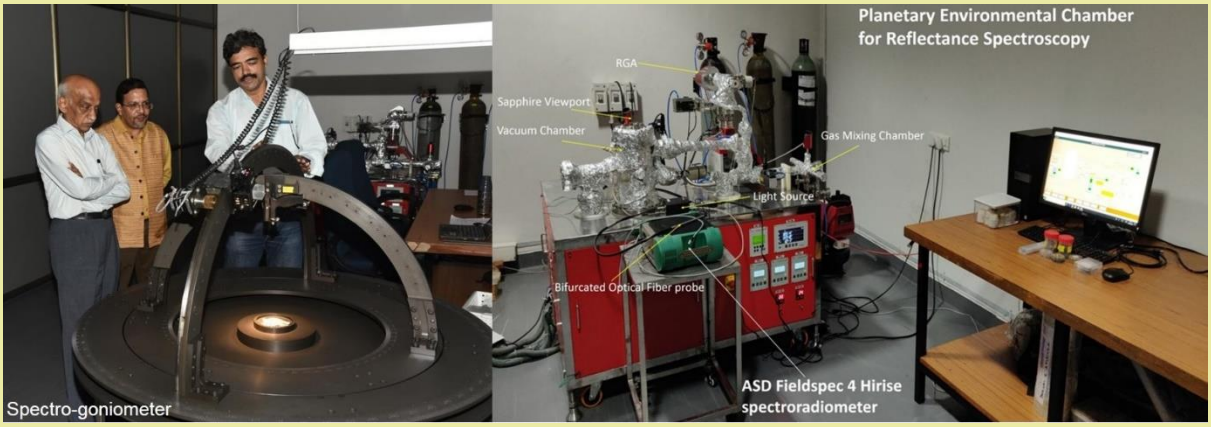

Figure: *The Planetary Remote Sensing Laboratory showing the spectro-goniometer (left) and the planetary environmental chamber with ASD Fieldspec spectroradiometer (right).*

Surface charge dissipation in permanently shadowed craters on Moon

(*S. K. Mishra and A. Bhardwaj*) (*11/05/2020*)

Sanjay K. Mishra

From an exploration perspective, the permanently shadowed craters (PSCs) on the Moon are of specific interest, as these cold traps might not only be confining the water, and hydrogen-based compounds, but also the pristine signature of evolution. The solar wind encounter with such large structures cause orographic effects, and the plasma expansion forms mini wakes behind the obstacle that makes the region electrically complex. The plasma neutrality breaks down near the crater flank edge that creates an electron-rich (ion free) region in the leeward side – this region may be extended to a few km. In the absence of any significant charge dissipation mechanism, this region might pose to an indefinite charge development, and its mitigation has been an open question so far. In addressing this, we propose that the fine particles lying on the surface act as field emission (FE) centres for the electron generation that can prevent the crater surface from acquiring large electric potential. For instance, PSC with ~100 nm dust, covering 1% of the surface within electron-rich region, may restrain surface at ~100's V negative potential. This conception is also pertinent with a fine irregular structure on the crater surface to dust scale (e.g., the amorphous ice within polar craters.

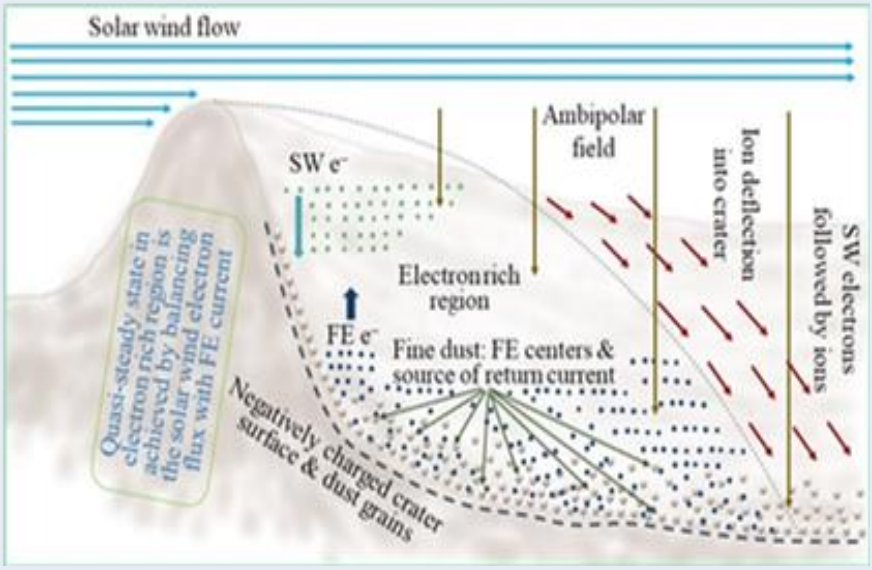

Figure: *Schematic shows the solar wind orographic effect: plasma expansion near the leeward surface of the polar obstacles (like PSCs).*

https://doi.org/10.1093/mnrasl/slaa082

Can Quasi-Periodic Gravity Waves Influence the Shape of Ice Crystals in Cirrus Clouds?

(Sourita Saha, N. Kondapalli, Som Sharma, P. Kumar and V. Joshi)(17/04/2020)

Sourita Saha

The present work, for the first time, unravels the impact of mesoscale gravity waves on the microphysical changes in cirrus clouds over Ahmedabad, a subtropical Indian region, using ground-based Raman lidar, Meteosat-7 satellite, WRF model simulations, and ERA5 reanalysis data sets. The cirrus clouds observed over the site were formed from the convective outflow of large - scale convergence zone extending from south - west to north - east Indian region. Signatures of very high frequency gravity waves with time periods ~40 and ~20 minutes, generated by this synoptic convergence, have been found in the cirrus clouds over the Raman lidar observational site. These clouds showed wavy patterns indicating that they were modulated by the upward propagating gravity waves. The wave-induced enhancement of moisture led to super-saturation and thereby modulating the ice crystals' size and shape in the cirrus clouds through depositional freezing. The ice crystals size increased, and they transformed to irregular shapes in the presence of wave activity. Ice crystals habits play a major role in the radiative budget of cirrus clouds. Therefore, the present work is novel and will have implications towards the uncertainties associated with cirrus clouds in both regional and global climate models.

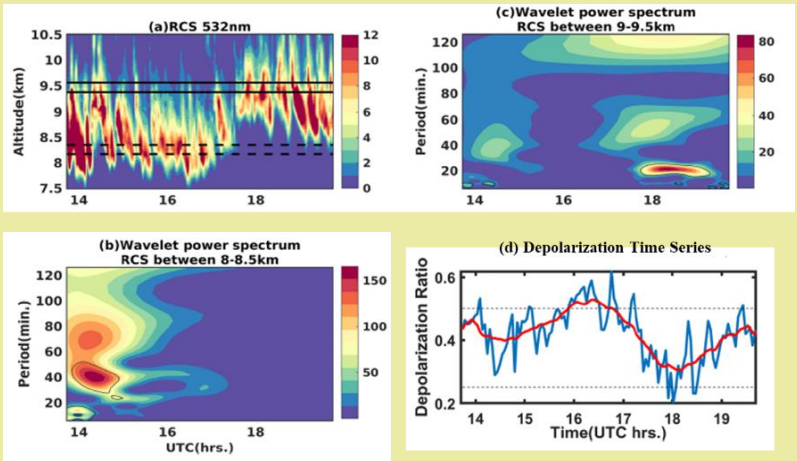

(Reference: S. Saha, N. Kondapalli, Som Sharma, P. Kumar, & V. Joshi, (2020), "Can Quasi Periodic Gravity Waves Influence the Shape of Ice Crystals in Cirrus Clouds?", Geophysical Research Letters (GRL), 47, e2020GL087909.

https://doi.org/10.1029/2020GL087909

Figure: *(a) Cirrus cloud patch (7.5–10.5 km) observed in 532-nm channel of RL. (b) Wavelet analysis of RCS spectrum between 8 and 8.5 km. (c) Wavelet analysis of RCS between 9 and 9.5 km. (d) 532 nm LDR time series (hourly mean shown in "red") along with threshold levels for different classes of ice crystal habits.*

Change in characteristics of water-soluble and water-insoluble brown carbon aerosols during a large-scale biomass burning

(Rangu Satish, Neeraj Rastogi, Atinderpal Singh, Darshan Singh)(12/06/2020)

Satish R. V.

Light absorbing organic aerosol (brown carbon, BrC) can significantly affect Earth's radiation budget and hydrological cycle. Biomass burning (BB) is among the major sources of atmospheric BrC. In this study, day/night pair of ambient $PM_{2.5}$ were sampled every day before (defined as T1), during (T2) and after (T3) a large-scale paddy-residue burning during October-November over Patiala, a site located in the northwestern Indo-Gangetic Plain (IGP). $PM_{2.5}$ concentration varied from ~90 to 500 μg m^{-3} with the average values of 154 ± 57, 271 ± 122, 156 ± 18 μg m^{-3} during T1, T2 and T3 periods, respectively, indicating the influence of BB emissions on ambient air quality. The absorption coefficient of BrC (b_{abs}) is calculated from the high-resolution absorption spectra of water-soluble and methanol-soluble organic carbon measured at 300 to 700 nm, and that at 365 nm (b_{abs_365}) is used as a general measure of BrC. The $b_{abs\_365\_Water}$ and $b_{abs\_365\_Methanol}$ ranged ~2 to 112 Mm^{-1} (avg: 37±27) and ~3 to 457 Mm^{-1} (avg: 121±108), respectively, suggesting a considerable presence of water-insoluble BrC. Contrasting differences were also observed in the daytime and nighttime values of $b_{abs\_365\_Water}$ and $b_{abs\_365\_Methanol}$. Further, the levoglucosan showed a strong correlation with K^+ (slope = 0.89 ± 0.06, R = 0.92) during the T2 period. We propose that this slope (~0.9) can be used as a typical characteristics of the emissions from paddy-residue burning over the IGP. Further at 365 nm, average relative atmospheric radiative forcing (RRF) for BrC_{Water} is estimated to be ~17%, whereas that of $BrC_{Methanol}$ ~62%, suggesting that BrC radiative forcing could be largely underestimated by studies those use BrC_{Water} only as a surrogate of total BrC.

https://doi.org/10.1007/s11356-020-09388-7

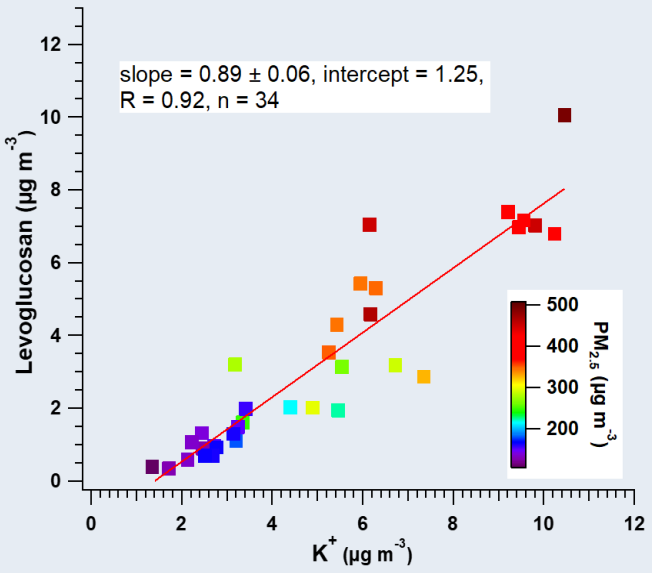

Figure: *Scatter plot between Levoglucosan and K^+, and the colored axis is $PM_{2.5}$ mass concentration for the samples collected during paddy-residue burning (T2 period).*

Linking pseudo-Dirac dark matter to radiative neutrino masses in a singlet-doublet scenario

(Partha Konar, Ananya Mukherjee, Abhijit Kumar Saha and, Sudipta Show)(29/07/2020)

Sudipta Show

The inability of the Standard Model (SM) of particle physics to cover the fascinating story of dark matter(DM) and neutrino mass is vastly known. Experiments to find out the nature and properties of DM through nuclear or electron recoils directly are continuing the search for ages. From a theoretical perspective, we keep building the guiding principles to support the experimental findings. We carry out such an exercise in a simple extended version of SM with a SU(2) singlet and a doublet fermions in this work. Here, the DM candidate is an admixture of the doublet's neutral component and the singlet. In such a minimalistic singlet doublet DM scenario, only the region below the black dotted line of the attached figure is allowed. The mixing angle is very constrained, and thus the DM is singlet-like, which hardly interacts with the SM. A tiny Majorana mass term for singlet fermion makes the DM pseudo-Dirac in nature. It can evade the strong spin-independent direct detection bound by suppressing the dark matter annihilation processes mediated by the neutral current. In that case, the mixing angle or the interaction rate of the DM can be enhanced substantially. The same Majorana mass term is remarkably associated with two or more singlet scalars that can provide the active neutrino mass. Hence, to summarize, we present a framework that offers the justification behind the null results at DM direct search experiments and the non-zero active neutrino mass simultaneously.

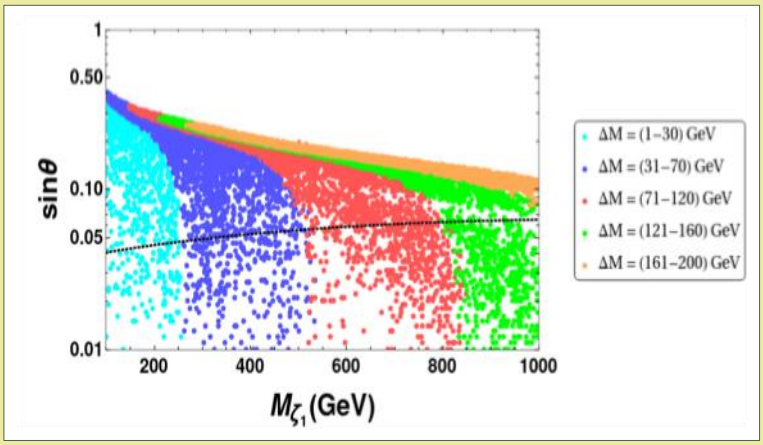

Figure: *Mixing angle vs. mass of the dark matter plot. The sine of the mixing angle and the dark matter mass is plotted along the Y-axis and X-axis. Here the color denotes the mas difference between the singlet and doublet.*

https://doi.org/10.1103/PhysRevD.102.015024

Geology of Grimaldi Basin on the Moon: Evidence for volcanism and tectonism during the Copernican period

(Tanu Singh and Neeraj Srivastava)(27/06/2020)

Tanu Singh

The availability of high-resolution datasets from various missions has greatly improved our understanding of the Moon by revealing volcanic and tectonic activities that have occurred in the recent past. We have found evidence of such events in the Grimaldi Basin, a Pre-Nectarian basin located near the western edge of the Oceanus Procellarum. Moon Mineralogy Mapper (M^3), FeO wt%, and TiO_2 wt % data have been used to study the compositional make-up of the Grimaldi mare basalt. Additionally, morphological studies and crater chronology have been carried out using moderate to very high-resolution images from Lunar Reconnaissance Orbiter (LRO) to decipher the geological evolution of the Grimaldi Basin. In this study, we have found that the basin experienced mare volcanism ~700 Ma ago in the south-central part resulting in the formation of ~80 m thick olivine bearing basalts with high FeO and TiO_2 content. These basalts are much younger than the earlier reported Late Phase (2.8 Ga – 1.2 Ga) mare basalts on the Moon. In addition, cross-cutting of small Copernican craters by fresh wrinkle ridges and lobate scarps has been observed at several places, suggesting that tectonic activities also occurred in the Grimaldi Basin during the past ~50 Ma-1 Ga.

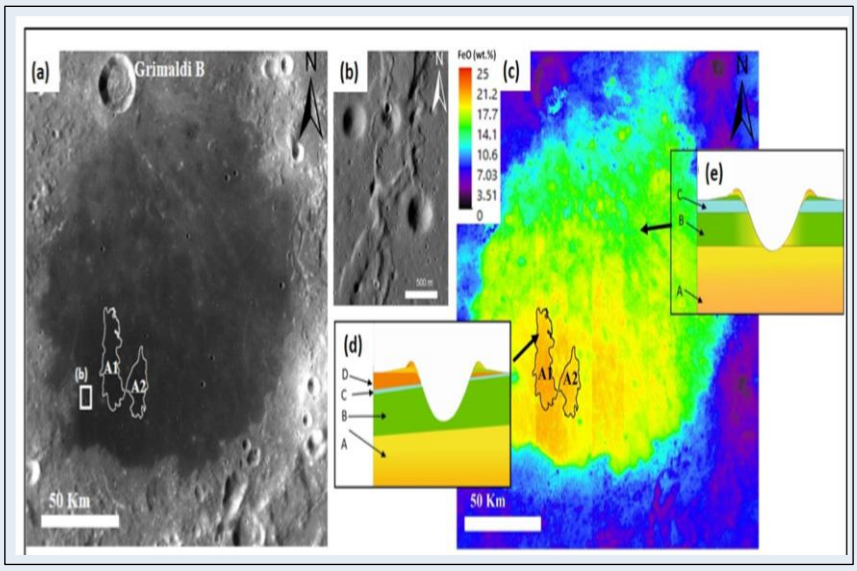

Figure : *(a) LROC WAC mosaic of Mare Grimaldi showing location of young mare unit A1 and A2 that formed ~700 Ma ago and location of the distorted craters enclosed within a square; (b) A blown-up view of the tectonically distorted small impact craters during recent times; (c) A FeO wt % map of the Mare Grimaldi showing the deciphered stratigraphic sequences (d) and (e). Here, A is the lowermost strata with high FeO content, B is the immediately overlying strata with intermediate FeO content, C is the ejecta unit of varying thickness deposited from crater Grimaldi B with very low FeO content, and D is the ~ 80 m thick uppermost strata with very high FeO content emplaced during the Copernican period.*

https://doi.org/10.1016/j.icarus.2020.113921

Forbidden atomic carbon, nitrogen, and oxygen emission lines in the water-poor comet C/2016 R2 (Pan-STARRS)

(S. Raghuram, D. Hutsemékers, C. Opitom, E. Jehin, A. Bhardwaj, and J. Manfroid)(01/03/2020)

Susarla Raghuram

The N_2 and CO-rich and water-depleted comet C/2016 R2 (Pan-STARRS) – hereafter "C/2016 R2" – is a unique comet for detailed spectroscopic analysis. We aim to explore the associated photochemistry of parent species, which produces different metastable states and forbidden emissions, in this cometary coma of peculiar composition. We reanalyzed the high-resolution spectra of comet C/2016 R2 obtained in February 2018 using the UVES spectrograph of the European Southern Observatory Very Large Telescope. Various forbidden atomic emission lines of [CI], [NI], and [OI] were observed in the optical spectrum of this comet when it was at 2.8 au from the Sun. The observed forbidden emission intensity ratios are studied in the framework of a couple-chemistry emission model. The model calculations show that CO_2 is the major source of both atomic oxygen green and red doublet emissions in the coma of C/2016 R2 (while for most comets it is generally H2O), whereas, CO and N_2 govern the atomic carbon and nitrogen emissions, respectively. Our modeled oxygen green-to-red-doublet and carbon-to-nitrogen emission ratios are higher by a factor of three than what is found from observations. These discrepancies could be due to uncertainties associated with photon cross sections or unknown production and/or loss sources. Our modeled oxygen green-to-red-doublet emission ratio is close to what is seen in observations when we consider an O_2 abundance with a production rate of 30% relative to the CO production rate. We constrained the mean photodissociation yield of CO, producing C(^{1}S) at about 1%, a quantity which has not been measured in the laboratory. The collisional quenching is not a significant loss process for N(2D) though its radiative lifetime is significant (~10 h). Hence, the observed [NI] doublet-emission ratio ([NI] 5198/5200) of 1.22, which is smaller than the terrestrial measurement by a factor 1.4, is mainly due to the characteristic radiative decay of N(^{2}D).

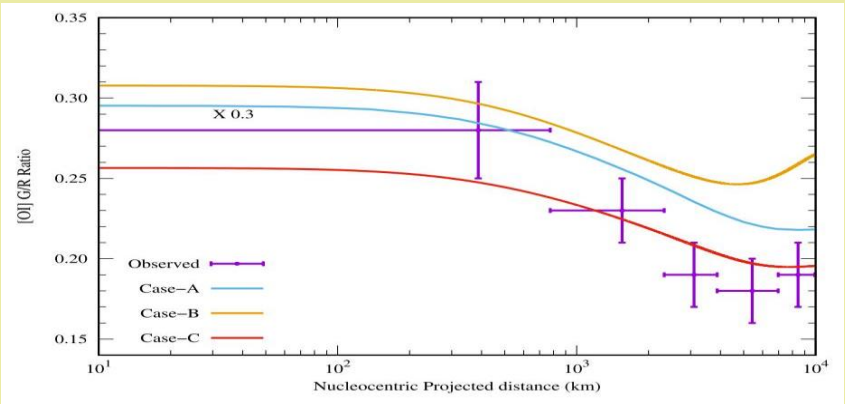

Figure: *Comparison between modeled and observed [OI] G/R emission ratios in C/2016 R2. For detail explanation for calculated emission ratios for Case-A to Case-C please see the publication.*

https://doi.org/10.1051/0004-6361/201936713

CO^+ first-negative band emission: A tracer for CO in the Martian upper atmosphere

(Susarla Raghuram and Anil Bhardwaj) (2/07/2020)

Recently, the Imaging Ultraviolet Spectrograph (IUVS) on board the Mars Atmosphere and Volatile EvolutioN (MAVEN) satellite observed CO^+ first-negative band limb emission in the Martian upper atmosphere. We aim to explore the photochemical processes in the Martian upper atmosphere, which drive this band emission. A photochemical model was developed to study the excitation processes of CO^+ first-negative band emission ($B^2\Sigma^+ \rightarrow X^2\Sigma^+$) in the upper atmosphere of Mars. The number density profiles of CO_2 and CO from two different models, namely, Mars Climate Database (MCD) and Mars Global Ionosphere-Thermosphere (MGIT), were used to determine the limb intensity of this band emission. By increasing the CO density by a factor of 4 and 8 in MCD and MGIT models, respectively, the modelled CO+ first-negative band limb intensity profile is found to be consistent with the IUVS/MAVEN observation. In this case, the intensity of this band emission is significantly determined by the ionisation of CO by solar photons and photoelectrons, and the role of dissociative ionisation of CO2 is negligible.

Since CO is the major source of the $CO^+(B^2\Sigma^+)$, we suggest that the observed CO^+ first-negative band emission intensity can be used to retrieve the CO density in the Martian upper atmosphere for the altitudes above 150 km.

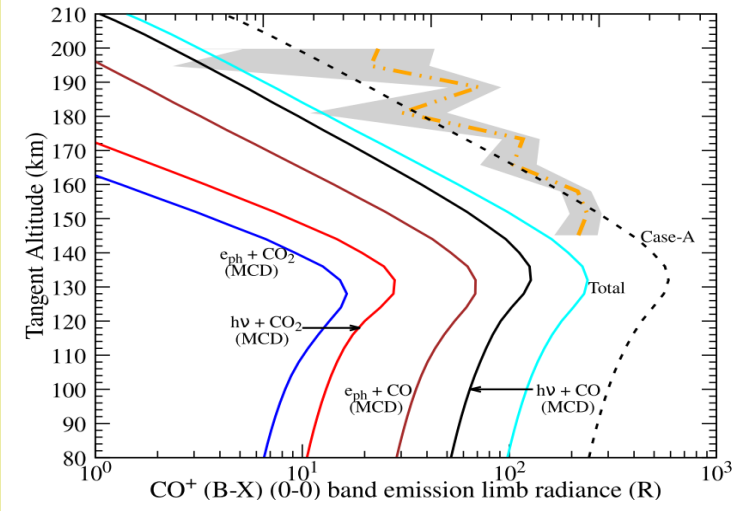

Figure: *Comparison between modelled CO^+ first-negative (0–0) band emission limb intensity profiles for different excitation mechanisms, using neutral densities from MCD models as well as the IUVS/MAVEN observation. Orange dash-doublet dotted curve and shaded area is IUVS observed mean emission intensity and its 1σ uncertainty.*

https://doi.org/10.1051/0004-6361/202038147

A photochemical model of ultraviolet atomic line emissions in the inner coma ofcomet 67P/Churyumov-Gerasimenko

(Susarla Raghuram and Anil Bhardwaj) (6/04/2020)

Alice ultraviolet spectrometer onboard Rosetta space mission observed several spectroscopic emissions emanated from volatile species of comet 67P/Churyumov-Gerasimenko during its entire escorting phase. The initial measured emission intensities, when the comet was at around 3 AU pre-perihelion, have been used to derive electron densities in the cometary coma assuming that H I and O I lines are solely produced by electron impact dissociative excitation of cometary parent species. We have developed a photochemical model for comet 67P/C-G to study the atomic hydrogen (H I 1216, 1025, & 973 Å), oxygen (O I 1152, 1304, & 1356 Å), and carbon (C I 1561 & 1657 Å) line emissions by accounting for major production pathways. The developed model has been used to calculate the emission intensities of these lines as a function of nucleocentric projected distance and also along the nadir view by varying the input parameters, viz., neutral abundances and cross sections. It is found that in comet 67P/C-G, with a neutral gas production rate of about 10^{27} s^{-1} when it was at 1.56 AU from the Sun, photodissociative excitation processes are more significant compared to electron impact reactions in determining the atomic emission intensities. Based on our model calculations, we suggest that the observed atomic hydrogen, oxygen, and carbon emission intensities can be used to derive H_2O, O_2, and CO, abundances, respectively, rather than electron density in the coma of 67P/C-G, when the comet has a gas production rate of 10^{27} s^{-1} or more.

doi.org/10.1016/j.icarus.2020.113790

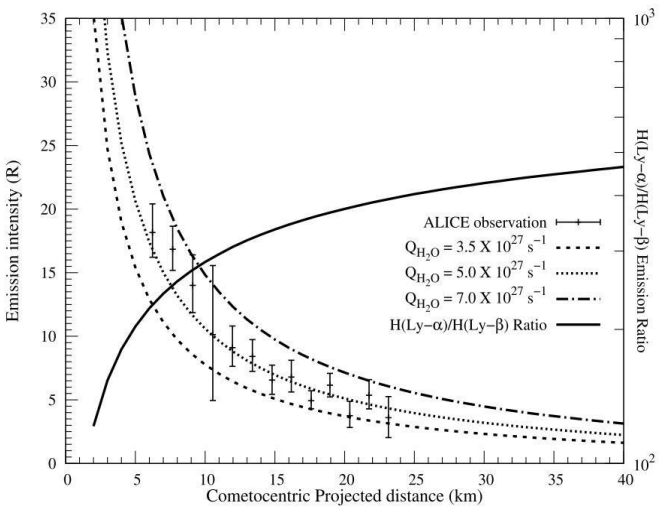

Figure: *Comparision between Modelled and Alice observed HI Lyman-β emission intensity profiles on comet 67P/C-G. Modelled emission intensity profiles are plotted as a function of comeotcentric projected distance for three different water production rates (Q H2O). Modelled HI Ly-α/Ly-β emission ratio is plotted on right y-axis.*

Aromatic compounds in a semi-urban site of western India: seasonal variability and emission ratios

(L. K. Sahu, Ravi Yadav, and Nidhi Tripathi) (24/06/2020)

Lokesh Sahu

The rapid urbanization of South Asia has resulted in increasing levels of various air pollutants adversely affecting the health and life expectancy of millions of people. Volatile organic compounds (VOCs) are emitted from both natural (biogenic) and anthropogenic sources, and play an important role in atmospheric chemistry. Among C_2-C_7 non-methane hydrocarbons (NMHCs), this is the first study of aromatic VOCs (benzene and toluene) at a semi-urban site of Udaipur in western India using almost year-round measurements from February to December 2015. The emission ratios of Δtoluene/Δbenzene indicate major contributions from vehicle exhaust in winter, biomass burning in early pre-monsoon, and evaporation of petrol and diesel fuels in late pre-monsoon. In wintertime, the higher concentrations of aromatic volatile organic compounds (VOCs) and CO were due to shallower boundary layer depths and transport from polluted Indo-Gangetic Plain. The ozone formation potential and propylene-equivalent concentration of aromatics were lower than those of alkanes and alkenes measured during the same study period. The composition of non-methane volatile organic compounds shows small change with the 'photochemical age' suggesting the contributions of several other sources in addition to vehicular exhaust. The study highlights major contributions of vehicle exhaust, but emissions from other sources such as biomass burning, industries, evaporative loss, and biogenic are also significant. Thus far, the impact of different VOCs with diurnally and seasonally varying concentrations contributing to the formation of ambient ozone is not clearly understood for many urban and semi-urban regions of India mainly due to the lack of comprehensive VOCs observations. One of our ongoing research programs is to conduct comprehensive observations of NMVOCs along with ozone, NOx, and CO using state-of-art instruments at different urban and semi-urban sites of India.

https://doi.org/10.1016/j.atmosres.2020.105114

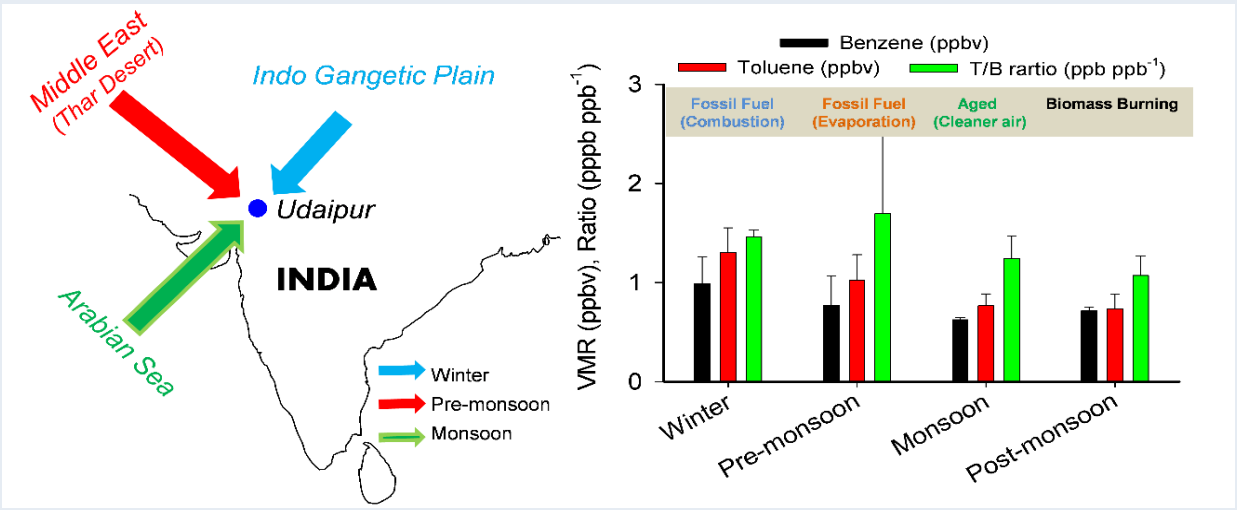

Figure: *Measurement site in Udaipur city is influenced by the winds from NE in the winter, NW in the pre-monsoon, and SW in the monsoon season. The seasonal comparison of mean mixing ratios of aromatic VOCs and toluene to benzene (T/B) ratio indicates the predominance of air masses influenced by different emission sources depending on the season.*

Processes governing the VIS/NIR spectral reflectance behavior of lunar swirls

(M. Hess, C. Woehler, M. Bhatt, A. A. Berezhnoy, A. Grumpe, K. Wohlfarth, A. Bhardwaj, and V. V. Shevchenko)(02/07/2020)

Megha Bhatt

Lunar swirls are curvilinear albedo markings of tens of kilometres size associated with magnetic anomaly regions but not related to distinct topography. We investigated six bright swirls associated with magnetic anomalies of variable strength using Chandrayaan-1 Moon Mineralogy Mapper (M3) hyperspectral image data. We examined the 3-µm absorption band generally ascribed to solar wind-induced OH/H2O and spectral trends in the near-infrared wavelength range at on-swirl and off-swirl locations. All examined swirls except the swirl in Mare Moscoviense exhibit a negative anomaly in 3-µm band depth with respect to the surrounding surface. Our spectral analysis results at on-swirl and off-swirl locations suggest that the spectral trends at on-swirl and off-swirl locations cannot always be explained by reduced space-weathering alone. To quantify observed spectral differences, the compaction-significance spectral index (CSSI) as a trade-off factor between reduced space weathering and regolith compaction is defined. Many locations at swirls have been found with high CSSI values indicating that regolith compaction is the major contributor to the observed spectral trends. The locations with low CSSI values represent spectral trends due to reduced space-weathering. The CSSI map of swirls (Fig. 1) supports the hypothesis that swirl formation is due to the interaction of the regolith with external influences, such as cometary gas. We propose that a combination of soil compaction possibly resulting from the interaction between the surface and cometary gas and subsequent magnetic shielding is able to explain all observed on-swirl vs. off-swirl spectral trends including the absorption band depth near 3-µm. Our results suggest that an external mechanism of interaction between a comet and the uppermost regolith layer might play a significant role in lunar swirl formation.

https://doi.org/10.1051/0004-6361/201937299

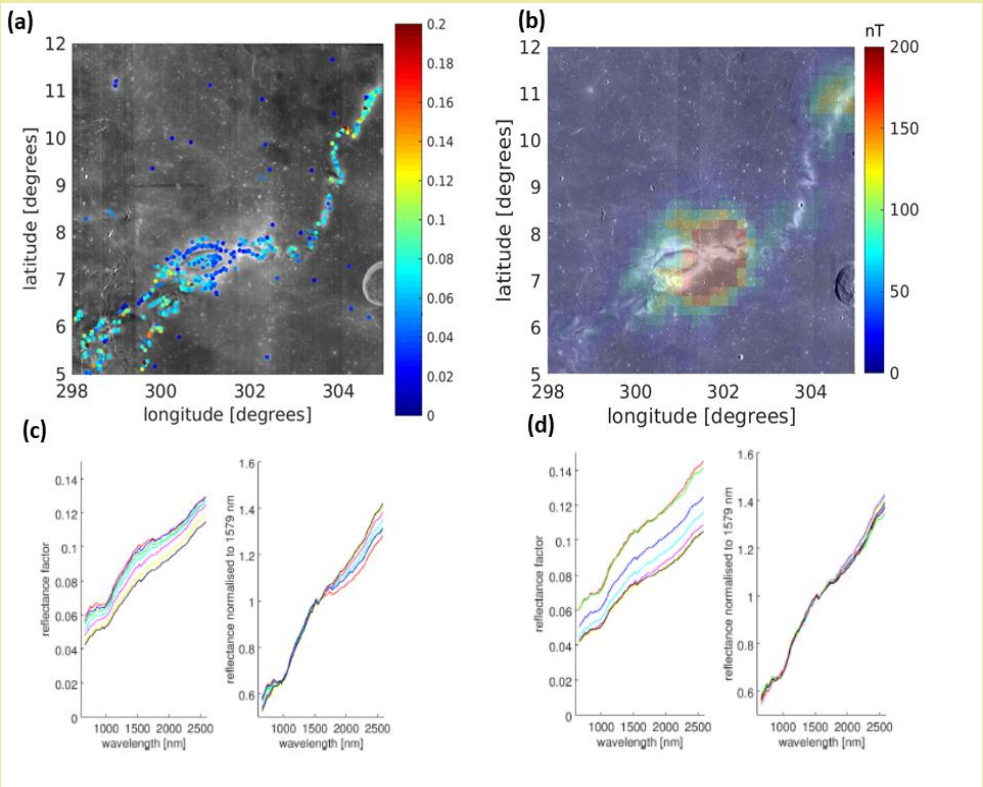

Figure: *Mare swirl Reiner Gamma (a) CSSI, overlaid on M3 reflectance at 1.579 µm. (b) images from the Lunar Reconnaissance Orbiter Camera Wide Angle Camera (LROC WAC; Robinson et al. 2010) mosaic with Kaguya magnetic flux density maps at surface level (Tsunakawa et al. 2015) as overlay. (c) and (d) Measured spectral trends from on-swirl to off-swirl locations for spectral pairs representing a spectral trend consistent with reduced space weathering and increased soil compaction, respectively.*

Evidence that magnetic-jerk accompanying major solar flares can drive seismic emissions in the sunspots

(Hirdesh Kumar and Brajesh Kumar)(08/07/2020)

Hirdesh Kumar

Recently., it was proposed that abrupt changes in the solar magnetic fields observed during the major flares can drive seismic waves in the Sun. Therefore, we have performed a detailed analysis of acoustic enhancements in sunspots accompanying M- and X-class solar flares and the associated changes in the magnetic fields. For this purpose, we have used high-resolution Dopplergrams and line-of-sight magnetograms at a cadence of 45 s, along with vector magnetograms at a cadence of 135 s obtained from HMI instrument on board the *SDO* space mission.
In addition, Hα observations from the GONG instrument and hard X-ray images from the *RHESSI* spacecraft were also utilized. Acoustic velocity power maps in 2.5–4 mHz band (*p*-modes) are constructed for pre-flare, spanning flare, and post-flare epochs for the identification of seismic emission locations in the sunspots. In the power maps, we have selected only those locations which are away from the flare ribbons and hard X-ray footpoints. These regions are believed to be free from any flare related artefacts in the observational data. We have identified concentrated locations of acoustic power enhancements in sunspots accompanying major flares. Our investigation provides evidence that abrupt changes in the magnetic fields and associated impulsive changes in the Lorentz force (known as 'magnetic-jerk') are the driving source for these seismic emissions in the sunspots during the flares. These seismic emissions in the sunspots are essential to study because these enhanced locations can provide better information about the deep dynamics in the active regions during the flare. In addition, since these 'magnetic-jerk' driven seismic waves can also propagate from photosphere to higher solar atmospheric layers along the magnetic field lines in the form of magneto-acoustic waves, hence these can contribute to the heating of the solar atmosphere.

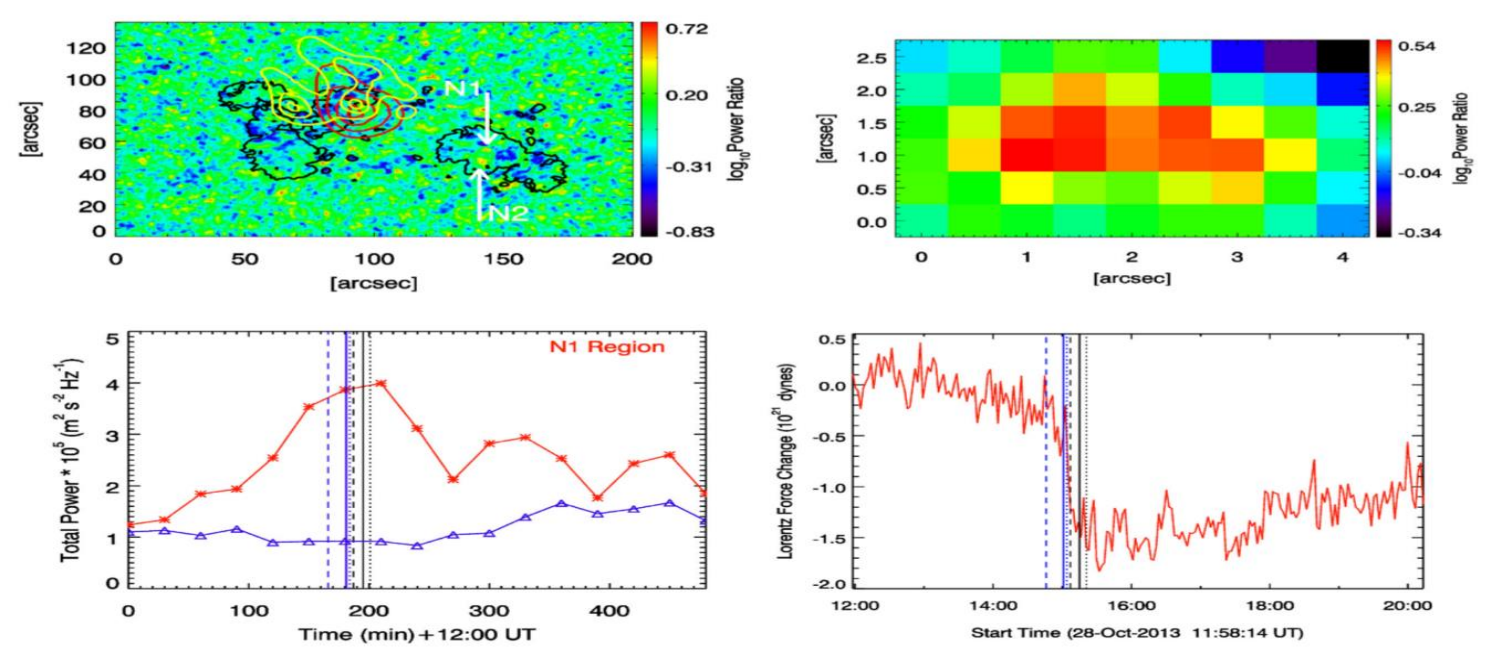

Figure: *A brief illustration of results obtained for the active region NOAA 11882. Top left panel: this illustrates the ratio of acoustic power maps estimated for spanning flare and pre-flare epochs in the 2.5–4 mHz band. Here, black contours represent the outer boundary of the sunspot penumbra, whereas the yellow contours represent flare-ribbon locations from the Hα observations from GONG. The red contours represent hard X-ray footpoints as observed in 12-25 keV band from RHESSI. Top right panel: illustrates the blow-up region of 'N1' enhanced location in the sunspot as indicated in the power map ratio. Bottom left panel: plots showing the temporal evolution of integrated acoustic power over the 'N1' location (red colour with asterisks) whereas that shown in blue colour with triangles represents evolution of total power in an unaffected region in the same sunspot. Bottom right panel: plot in red colour shows the temporal evolution of change in horizontal component of Lorentz force in the 'N1' location. The dashed, solid, and dotted blue and black vertical lines represent the onset, peak, and decay time of M2.7 and M4.4-class flares, respectively.*

10.1093/mnras/staa1974

B. Sivaraman

Astrobiology is one of the interdisciplinary areas of science that is rapidly evolving and has the potential to reveal the mystery that shrouds the Origin of Life. The research carried out in India in this trans disciplinary field is developing, and there is a lot of interest to engage in astrobiology research at various levels. There are a few courses works in astrobiology taught in academic institutions. Many students are interested in carrying out short and long term projects in astrobiology.

The unforeseen circumstances that we are facing now due to COVID19 pandemic has heavily affected the summer projects at various levels, especially for emerging research area, such as astrobiology. It is imperative to keep up the momentum. Hence, we are organizing a webinar series of astrobiology lectures from international and national academics carrying out astrobiology research and teaching.

The series of talks had begun on 02 June 2020 and will go on for a few months. Link to webinar registration can be found in the PRL webinar page. Registered participants will get an email reminder with a link to the webinar a day before the scheduled talk.

More details are available at: *https://www.prl.res.in/prl-eng/activity/astrobiology_webinar*
The webpage also includes link to register for the webinar and to watch it live on YouTube. Archive to the previous talks are placed at the recorded video section.

Comet NEOWISE Spotted from PRL Hill View, Mount Abu Campus

S N Mathur

Comets are cosmic snowballs of frozen gases, rock and dust that orbit the Sun. When a comet's orbit brings it close to the Sun, it heats up and spews dust and gases into a giant glowing head.

"Since 21st – 23rd July 2020 the comet “NEOWISE” was visible near Ursa Major, which is also the Saptarshi Mandal at a height of 30 -40 degrees and was visible for an hour from our site. Now it will fade away very fast and will not be visible to the unaided eye. A pair of binoculars or a small telescope, enhance its visibility,"

It was a rare opportunity to catch a magical glimpse of this ancient ice ball from PRL Hill View Campus, Mount Abu, Rajasthan, India during peak monsoon season. Fortunately, sky at Mount Abu on 21st & 23rd July 2020 was very clear during the event time.

By using Canon E - 600 DSLR Camera, we took many exposures (more than 300 exposures) from 10 to 30 seconds.

PRL Mount Abu Staff & there family members enjoyed the event in such a long COVIND -19 Pandemic Lockdown & Unlock down situation.

Comet C/2020 F3, also known as NEOWISE, was discovered earlier this year by NASA’s Near-Earth Object Wide-field Infrared Survey Explorer telescope. While the comet was visible in the early morning hours before July 12, sky we could witness NEOWISE after sunset until around 8:15 to 9:15 pm in the north-western direction. An excellent opportunity to witness comet NEOWISE, which will not be visible for the next 6,800 years, is on July 23 as it will be closest to Earth.

Awards & Honours

- Arvind Singh (Associate Professor , GSDN) has been selected for the MoES Young Researcher award for his outstanding work in the field of Earth System Science. This award carries an award amount of Rs. 50,000/- and a citation.
- Publication entitled, "A New Tool for Predicting the Solar Cycle: Correlation Between Flux Transport at the Equator and the Poles" authored by Susanta Kumar Bisoi & P. Janardhan in Solar Physics has been featured as a news report in the 25th July issue of Current Science.

PRL Congratulates family members conferred with awards and honours

Obituaries

Late Shri R.C. Solanki Assistant Administrative Officer ADM-CN	
Date of Birth	07.10.1949
Date of retirement	31.10.2009
Date of Death	30.06.2020

Late Shri Jayantilal S Patel Helper-C ADM-AC	
Date of Birth	07.05.1942
Date of retirement	31.05.2002
Date of Death	01.07.2020

PRL mourns the demise of our former employees and fondly remembers their contribution to PRL. We pray for the wellbeing of their bereaved families. May their souls rest in peace.

The Editorial Team

Bijaya Sahoo

A.Shivam

Deekshya Sarkar

Pragya Pandey

Rohan Louis

Garima Arora

Prashant Jangid


PRL Newsletter wishes you a
Happy Independence Day
भौतिक
अनुसंधान
प्रयोगशाला